PHILOSOPHICAL TRANSACTIONS OF THE ROYAL SOCIETY B BIOLOGICAL SCIENCES

Dynamics of Arthropod Filiform Hairs. IV. Hair Motion in Air and Water

Raghuram Devarakonda, Friedrich G. Barth and Joseph A. C. Humphrey

Phil. Trans. R. Soc. Lond. B 1996 **351**, 933-946
doi: 10.1098/rstb.1996.0086

Dynamics of arthropod filiform hairs. IV. Hair motion in air and water

RAGHURAM DEVARAKONDA[1], FRIEDRICH G. BARTH[1]* AND JOSEPH A. C. HUMPHREY[2]

[1] *Biozentrum, Institut für Zoologie, Universität Wien, Althanstr. 14, A-1090 Wien, Austria*
[2] *Department of Aerospace and Mechanical Engineering, University of Arizona, Tucson, Arizona 85721, U.S.A.*

CONTENTS

PAGE
1. Introduction 933
2. Procedure and mathematical model 934
3. Results 935
  (*a*) *Flow media effects* 935
  (*b*) *Hair parameter effects* 939
  (*c*) *Hair substrate and flow configuration effects* 942
4. Discussion 943
  (*a*) *Boundary layer thickness* 943
  (*b*) *Reynolds and Strouhal numbers* 943
  (*c*) *Hair length* 943
  (*d*) *Hair diameter* 944
  (*e*) *Frequency* 944
References 945

SUMMARY

Filiform cuticular hairs responding to movements of the surrounding medium are widespread mechanoreceptors in both terrestrial and aquatic arthropods. In this study we compare the motion response of such hairs to sinusoidal oscillations in air and in water, by applying a previously developed mathematical model (Humphrey *et al.* 1993). In addition to the physics underlying stimulus uptake in the two media, the effects of changing the values of various geometrical and mechanical parameters characterizing a hair in motion are studied. The differences in the hair motion response for an identical hair in air and water are indeed considerable. They are mainly due to the difference in dynamic viscosity of the two media, which entails an overriding contribution of the 'virtual (added) mass' to the effective inertia of the hair in water. The large effective moment of inertia for a hair in water enables it to perform as a displacement sensor at low frequencies and as an acceleration sensor at high frequencies. Hairs in air function as displacement, velocity and acceleration sensors over different frequency ranges. 'Boundary layer thickness' is smaller by a factor of 0.22 in water than in air. As a consequence of this and of the proportionately larger drag force in water, we may expect shorter hairs among the receptors serving the uptake of hydrodynamic stimuli than among those dealing with aerodynamic stimuli. This, in fact, seems to be the case. Whereas hair length greatly influences a hair's mechanical sensitivity both in air and water, hair diameter is of only minor importance in water. Our results point to several important differences between the hairs in the two media regarding their 'tuning'. Mainly due to the importance of virtual mass, resonance frequencies for the same hair are much lower in water than in air. Whereas hairs in air are more sensitive to changes in hair length regarding resonance frequency, hairs in water are the more sensitive regarding the amplitude of motion. Underlining the general tendency found for the geometrical hair parameters, changing the spring stiffness and torsional damping influences a hair's tuning much more in air than in water. Our analysis suggests that the evolutionary pressures on both the morphological and the mechanical properties characterizing arthropod (or any other) filiform hair receptors must have been bigger in air than in water.

1. INTRODUCTION

Mechanosensitivity may be the oldest of all sensitivities of living cells and organisms. Mechanosensitive ion channels are now known throughout the phyla from bacteria to vertebrates and their widespread and longstanding occurrence is thought to be linked not only to sensory functions in the classical sense, but also to such general processes as volume regulation and osmoregulation.

---

* Author to whom correspondence should be addressed.

Regarding the sensory ecology of mechanoreceptive systems like filiform hairs and their role in guiding the behaviour of whole animals, questions of stimulus uptake and stimulus transformation at the precellular level by the receptor's auxiliary structures, are of particular relevance. As has been amply shown, it is the difference in these auxiliary structures which is primarily responsible for the specialization of a mechanoreceptor to a particular type of stimulus. Considering the number of Arthropod species, the number of individuals representing each species and the richness of their cuticular mechanoreceptive hair supply, hairs are likely to be the most common auxiliary structures in existence. With different modifications of hairs a large spectrum of stimuli can be perceived, ranging from touch to the reception of the slightest movements of the surrounding medium. Building on the existing literature (Tautz 1977, 1979; Fletcher 1978; Shimozawa & Kanou 1984; Kämper & Kleindienst 1990) we have recently extended the fluid mechanical theory of arthropod hairs (Humphrey *et al.* 1993) and taken the trichobothria of a large wandering spider (*Cupiennius salei* Keys.) to compare in detail the measured properties of hair and air motion with the values predicted numerically by theory (Barth *et al.* 1993). There was very good agreement between the two, and our work has served to clarify various omissions and correct some inaccuracies existing in the literature.

This paper carries our analysis one major step further by comparing the motion of hairs in two rather different media, air and water. Like the reception of aerodynamic stimuli, the reception of hydrodynamic stimuli by cuticular hairs is very widespread and, in particular, described for marine and freshwater decapod crustaceans (Laverack 1962; Wiese 1976; Derby 1982; Breithaupt & Tautz 1990). Because our theoretical considerations (Humphrey *et al.* 1993) are of a very general nature they can be applied not only to different hair morphologies and hair mechanics, but also to different media. This analysis predicts a number of media-dependent differences in the physics of stimulus uptake which we expect to be reflected in the structure and mechanics of the hairs or hair-like structures actually mediating sensitivity to aerodynamic and hydrodynamic stimuli, respectively.

An overview of the investigation methodology is followed by the presentation of results along with comments from a physics point of view. The discussion section focuses on the biological perspective of the results.

2. PROCEDURE AND MATHEMATICAL MODEL

As detailed in Humphrey *et al.* (1993), the structure of the hair-like object is approximated by a circular cylinder of diameter d and length L. The mechanical characteristics for a hair are the torsional spring S and damping R constants for the pivoting joint at the base of the hair. The values for d and L can be obtained from the geometry of the hair. However, to determine R and S, dynamic experiments must be conducted (Kämper & Kleindienst 1990) and the data analysed using the theory derived in Humphrey *et al.* (1993). Such an experimental dataset is not available for spider trichobothria or crustacean hairs. However, by using a trial-and-error method based on hair amplitude and frequency data, Barth *et al.* (1993) obtain values of S and R for spider trichobothria of which the former are comparable in magnitude to values of S corresponding to cricket cerci. As a result, in this study values for R and S are taken from the analysis of the experimental dataset corresponding to filiform hairs on the cricket cerci (Kämper & Kleindienst 1990; Humphrey *et al.* 1993).

Our investigation includes a sensitivity study of the effects due to changing the hair parameters L, d, S and R on the hair's mechanical response in the two media (air and water). This is of help in estimating the range of values taken by these parameters for crustaceans, spiders and other terrestrial arthropods. In addition, the study discusses issues pertaining to the role of a hair as a displacement, velocity and acceleration sensor.

Central to the theoretical analysis is the equation representing the conservation of angular momentum for a hair-like object (Humphrey *et al.* 1993):

$$I\ddot{\theta} = -R\dot{\theta} - S\theta + T_{\mathrm{D}} + T_{\mathrm{VM}}, \qquad (1)$$

where I (kg m^2) is the moment of inertia of the hair with respect to the axis of rotation, R (N m s rad^{-1}) is the damping constant at the base of the hair, S (N m rad^{-1}) is the torsional restoring constant at the base of the hair, θ (rad) is the angular displacement of the hair about its base, and the superscript dots on θ denote differentiation with respect to time. T_{D} (N m) is the torque arising due to fluid-induced stress forces acting along the length of the hair, and T_{VM} (N m) is the torque associated with the added (or virtual) mass of fluid which at any instant must be displaced along with the hair.

The torques T_{D} and T_{VM} are obtained by integrating the fluid-induced drag and added mass forces acting along the length of the hair. These forces are calculated using Stokes' (1851) theory for a fluid oscillating perpendicular to a cylinder. The conditions to be satisfied for Stokes' (1851) theory to apply are: $L/d \gg 1$, Re $(= V_{\mathrm{r}}\, d/2/\nu) \ll 1$, and s $(= d/4(2\pi f/\nu)^{0.5}) \ll 1$; where f is the frequency of flow field oscillation, ν $(= \mu/\rho)$ is the kinematic viscosity, μ the dynamic viscosity, ρ the density of the fluid, and V_{r} $(= V_{\mathrm{tip}}\text{-}L\ \dot{\theta})$ is the relative velocity between the fluid adjacent to the hair tip (V_{tip}) and the hair tip ($L\dot{\theta}$). These conditions are satisfied by all the hair-medium combinations studied in this work. For a detailed listing of the equation due to Stokes' (1851), the reader is referred to Humphrey *et al.* (1993).

In their equation (19) Humphrey *et al.* (1993) provide a nondimensional representation of the motion of a hair in terms of the hair and fluid medium parameters. (Note two printing errors in equation 19 of Humphrey *et al.* (1993): the π_2 term should be written as π^2 and the quantity V_{F}^{*} in the last term should be written as $\dot{V}_{\mathrm{F}}^{*}$ as in equation 2.)

A modified version of the equation, extended here to include the virtual mass density term that is generally not negligible in water, is given by:

$$\ddot{\theta}^* + \frac{R_{\text{eff}}}{I_{\text{eff}}\omega}\dot{\theta}^* + \frac{S}{I_{\text{eff}}\omega^2}\theta^* = \frac{4\pi\mu G L^3}{I_{\text{eff}}\omega}\int_0^1 V_{\text{F}}^* \eta d\eta - \left(\frac{\pi^2 \mu G L^3}{I_{\text{eff}}\omega g} - \frac{\pi\rho\,(d/2)^2 L^3}{I_{\text{eff}}}\right)\int_0^1 \dot{V}_{\text{F}}^* \eta d\eta, \quad (2)$$

where $\ddot{\theta}^* = \ddot{\theta} L/\omega U_{\text{o}}$, $\dot{\theta}^* = \dot{\theta} L/U_{\text{o}}$, $\theta^* = \theta L\omega/U_{\text{o}}$, $\eta = y/L$, $V_{\text{F}}^* = V_{\text{F}}/U_{\text{o}}$, $\dot{V}_{\text{F}}^* = \dot{V}_{\text{F}}/\omega U_{\text{o}}$, $\omega = 2\pi f$; I_{eff} is the effective moment of inertia due to the hair and the added mass of the medium; R_{eff} is the effective damping due to friction at the base of the hair and by fluid viscosity; G and g are parameters originating in Stokes' (1851) drag analysis and are functions of s. The reader is referred to Humphrey *et al.* (1993) for the expressions defining I_{eff}, R_{eff}, G and g. The variable y is the distance along the hair with origin at the hair base, U_{o} is the far field uniform velocity oscillation amplitude, V_{F} is the local fluid velocity and $\dot{V}_{\text{F}}$ is the local fluid acceleration.

Equation (2) can be rewritten as:

$$\ddot{\theta}^* + G_{\text{R}}\dot{\theta}^* + G_{\text{S}}\theta^* = G_{\text{D}}\int_0^1 V_{\text{F}}^* \eta d\eta - G_{\text{VM}}\int_0^1 \dot{V}_{\text{F}}^* \eta d\eta, \quad (3)$$

with the following definition of dimensionless parameters,

$$G_{\text{R}} = \frac{R_{\text{eff}}}{I_{\text{eff}}\omega},\ G_{\text{s}} = \frac{S}{I_{\text{eff}}\omega^2},\ G_{\text{D}} = \frac{4\pi\mu G L^3}{I_{\text{eff}}\omega},\ G_{\text{VM}} = \left(\frac{\pi^2 \pi G L^3}{I_{\text{eff}}\omega g} - \frac{\pi\rho\,(d/2)^2 L^3}{I_{\text{eff}}}\right). \quad (4)$$

The relative values of the nondimensional parameters G_{R}, G_{S}, G_{D} and G_{VM} (which represent damping, stiffness, drag and virtual mass, respectively) dictate the motion of the hair. Individually, they represent the scaled order of magnitude of the terms they modify thus allowing an unambiguous qualitative interpretation of the physics of hair motion. The terms inside the integrals of equation (3) represent the fluid velocity and acceleration along the length of the hair. Equation (3) was accurately solved using the fourth-order Runge-Kutta technique (for further details regarding equation (3) and the solution procedures see Humphrey *et al.* 1993).

Unless otherwise mentioned, the nominal values for the geometrical and mechanical characteristics of a hair in this study are: $d = 7$ μm, $L = 500$ μm, $S = 4 \times 10^{-12}$ N m rad^{-1}, and $R = 0$ N m s rad^{-1}. These values for parameters representing hair geometry and mechanical characteristics are considered representative for a hair in air (Barth *et al.* 1993). In the absence of real R values we imply a system with zero mechanical damping ($R = 0$) associated with the mechanics at the articulation of the hair. R effects are studied separately. In addition, the substrate for the hair is taken to be flat; Humphrey *et al.* (1993) show that the flat substrate configuration accurately represents the substrate-medium oscillation orientation wherein the longitudinal axis of the cylindrical substrate (for example, a spider leg) is parallel to the flow oscillations. The effects of other substrate-medium configurations on hair motion are discussed later in the paper.

The flow oscillation in the region far from the hair and the substrate is prescribed as a pure sinusoidal function of time whose amplitude (U_{o}) is fixed at 5 mm s^{-1} with a frequency range $0.1 \leqslant f \leqslant 500$ Hz. The frequency range includes the frequencies contained in natural signals (Tautz 1979; Bleckmann 1994).

Calculations are performed for an identical hair (same values for d, L, S and R) in air and in water, and the responses of the hair in the two media are compared. The values for the fluid medium properties at 27 °C are: $\rho_{\text{air}} = 1.1614$ kg m^{-3}, $\mu_{\text{air}} = 1.85 \times 10^{-5}$ kg m^{-1} s^{-1} ($\nu_{\text{air}} = 1.59 \times 10^{-5}$ m^2 s^{-1}); $\rho_{\text{water}} = 995.6$ kg m^{-3}, $\mu_{\text{water}} = 8 \times 10^{-4}$ kg m^{-1} s^{-1} ($\nu_{\text{water}} = 8 \times 10^{-7}$ m^2 s^{-1}). The density for the hair is taken to be, $\rho_{\text{hair}} = 1100$ kg m^{-3}.

3. RESULTS

(*a*) *Flow media effects*

Equation (3) shows that the hair response depends on the fluid velocity and acceleration profiles (boundary layer) established on the substrate, and on the values for G_{R}, G_{S}, G_{D} and G_{VM} (hair motion parameters). Thus, it will be useful first to understand these functions before analysing the hair motion in the two media.

(i) *Boundary layer*

For the present case of a flow oscillating over a flat substrate, the thickness of the boundary layer, δ, is given by $\delta = 2.54\ (\nu/f)^{0.5}$ (see Humphrey *et al.* 1993) where ν is the kinematic viscosity (μ/ρ), and f the flow oscillation frequency. The value of δ delimits the region of flow affected by the presence of the substrate due to viscous effects. For distances larger than δ from the substrate the flow field can be taken as uniform. Because $\nu_{\text{water}} < \nu_{\text{air}}$, for fixed f the value of δ will be about 4.5-fold smaller in water than in air. Further, in either medium δ decreases with increasing f. The smaller values of ν and δ for water imply that information concerning the existence of the substrate diffuses a smaller distance away from the substrate surface in water as compared to air.

Figure 1 shows typical velocity profiles for water and air at the instant in an oscillation cycle corresponding to the far field velocity at its maximum value (calculations see Humphrey *et al.* 1993). Values of δ were estimated from these data (figure 2*a*). As predicted, δ decreases with increasing f, and is smaller in water than in air. For all conditions being equal, a hair of fixed length penetrates further into (or past) the boundary layer in water than the corresponding boundary layer in air.

For a cylinder of diameter D (representing an appendage such as a leg) oriented parallel to the plane of the flow field oscillations, Humphrey *et al.* (1993) show that if the condition $fD^2/\nu > 20/\pi$ is satisfied, then the boundary layer thickness estimated for a flat substrate is applicable. Figure 2*b* shows the minimum

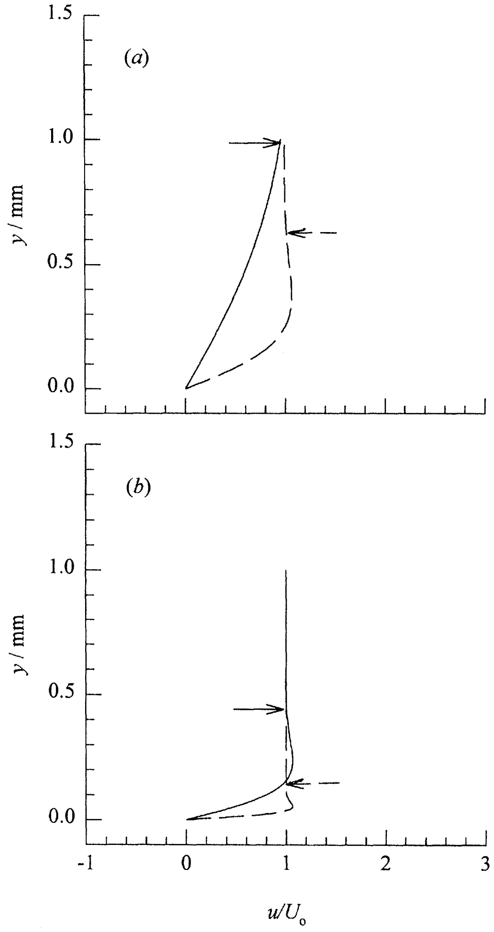

Figure 1. Flow media effects: velocity profiles at time $wt = \pi/2$ in air (solid line) and water (dashed line) for a flow field oscillation frequency of (*a*) 10 Hz; and (*b*) 500 Hz. The substrate is a flat surface.

values of f required for a given value of substrate diameter, D, to satisfy the condition. Thus, for example, an appendage larger than 2 mm in diameter in water must be exposed to a flow with $f \geqslant 1.3$ Hz. In contrast, the same appendage in air would require $f \geqslant 25$ Hz. For (D, f) pairs not satisfying the condition, the boundary layer is thinner than estimated using the flat substrate formula.

(*ii*) *Hair motion parameters*

G_R, G_S, G_D and G_{VM} change with flow field oscillation frequency. The values shown in figure 3 are for a hair with $L = 500$ µm, $d = 7$ µm, $R = 0$ N m s rad^{-1} and $S = 4 \times 10^{-12}$ N m rad^{-1} in air and in water. G_S differs markedly between the two media at frequencies below 100 Hz. G_R, G_D and G_{VM} vary similarly with frequency in both air and water without showing the large difference between the two media displayed by G_S. Whereas the sensitivity to changing frequency is more pronounced in air than in water below 200 Hz, it is almost the same in the two media beyond 200 Hz.

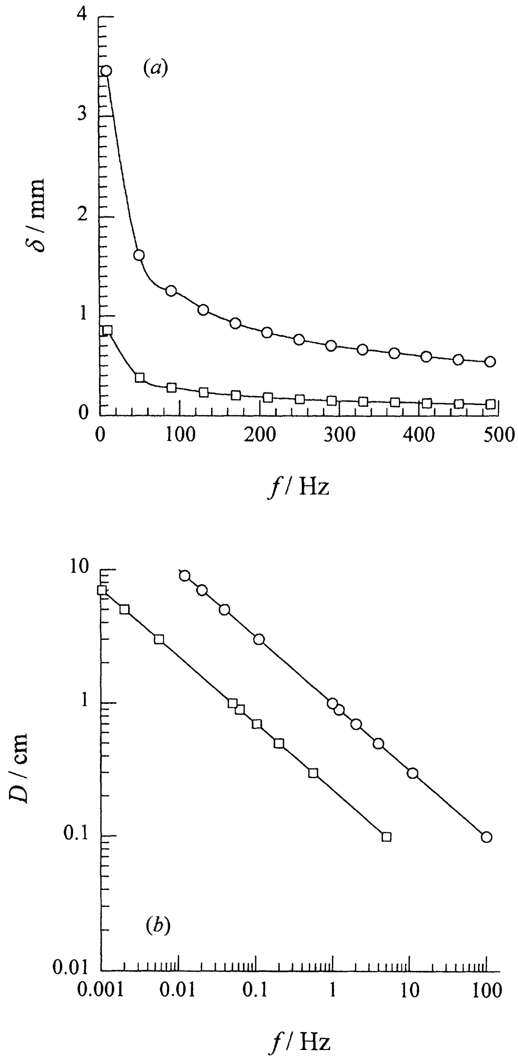

Figure 2. Flow media effects: (*a*) boundary layer thickness (δ) as a function of flow oscillation frequency for a flat substrate in air (circles) and water (squares). (*b*) Plot of $fD^2/\nu = 20/\pi$ in air (circles) and water (squares). The graph shows the conditions under which a cylinder of diameter D in parallel orientation with the plane of flow field oscillations can be accurately approximated by a flat substrate. The approximation is valid for f and D values contained in the region that is on the right side of the plotted lines, and invalid on the left side. In water, the approximation is valid at lower f and D values than in air.

The expressions for G_R, G_S, G_D and G_{VM} given in equation (4) depend on I_{eff}, the effective moment of inertia. I_{eff} depends on fluid density, viscosity, oscillation frequency, hair diameter and length. From the expression for I_{eff} ($= I_{VM} + I_{hair}$) in Humphrey *et al.* (1993), it can be shown that, for the same hair in air or water, the effective moment of inertia is given by:

$$I_{eff} = \frac{C_1 \mu}{[g^2 + (\pi^2/4)]\,\omega} + C_2 \rho_{fluid} + I_{hair}, \qquad (5)$$

where $C_1(L)$, and $C_2(d,L)$ are constants when the values for the parameters in parentheses are fixed. The first two terms on the right hand side of equation (5) together represent I_{VM}, the moment of inertia due to virtual mass. The moment of inertia due to the hair, I_{hair}, is independent of the properties of the fluid medium and, hence, this term has the same value in both air and water. Any differences in the values of I_{eff} for a hair when in air or in water must arise from differences in the values for I_{VM}.

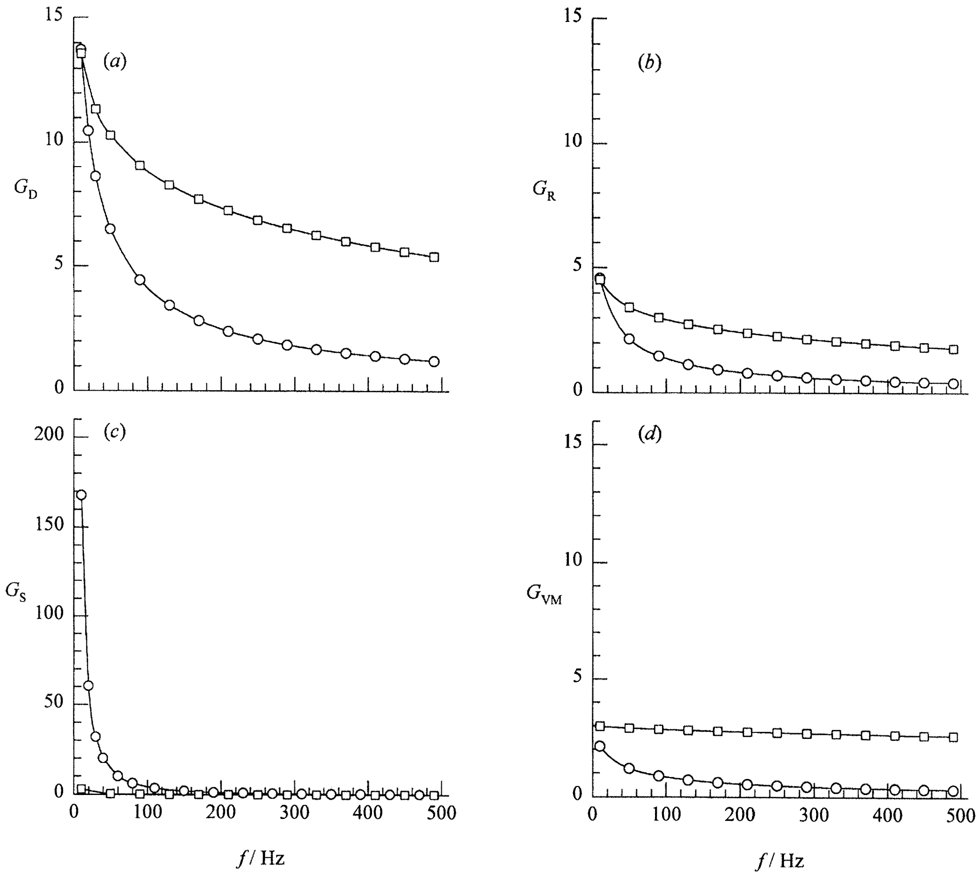

Figure 3. Flow media effects: plots of nondimensional coefficients appearing in the equation of motion for the hair (equation 3) for a hair of $L = 500\ \mu\text{m}$, $d = 7\ \mu\text{m}$, $S = 4 \times 10^{-12}$ N m rad^{-1}, $R = 0$ N m s rad^{-1} in air (circles) and water (squares). (*a*) G_D, drag coefficient; (*b*) G_R, damping coefficient; (*c*) G_S, spring coefficient; and (*d*) G_{VM}, virtual-mass coefficient.

Table 1. *Values of* C_1 *and* C_2 *in equation* (5) *for two hair diameters*

	$d = 7\ \mu\text{m}$	$d = 14\ \mu\text{m}$
C_1 (m^3)	4.11×10^{-10}	4.11×10^{-10}
C_2 (m^5)	1.60×10^{-21}	6.41×10^{-21}

Table 1 gives values of C_1 and C_2 for two hairs of $L = 500\ \mu\text{m}$ and diameters $d = 7\ \mu\text{m}$ and $14\ \mu\text{m}$. Given that $\rho_{\text{air}} = 1.1614$ kg m^{-3} and $\rho_{\text{water}} = 995.6$ kg m^{-3} it can be inferred that for the same values of C_2 the second term on the right hand side of equation (5) will have more influence in water than in air. However, from the values of I_{VM} in table 2, it can be seen that the contribution of the second term on the right hand side of equation (5) is quite small, even in water. Thus, the differences in the values of I_{VM} (and therefore in the values of I_{eff}) for the two media are mainly due to the first (viscosity-related) virtual mass term on the right hand side of equation (5).

For the same frequency, ω, media dependent differences in the first term on the right hand side of equation (5) arise due to differing values of dynamic viscosity, μ, and g: a parameter which depends logarithmically on kinematic viscosity ν (μ/ρ) and hair diameter d (Humphrey *et al.* 1993). Noting that a change in medium produces a proportionately larger change in the numerator of this first term (through the direct dependence on μ) than in its denominator (through the logarithmic dependence of the ν in g), it can be concluded that for air and water oscillating at the same frequency differences in the values for I_{VM} are mainly due to the differences in the values of dynamic viscosity (μ). This is a rather striking finding since intuition would tend to attribute the differences in I_{VM} to the very large differences in density between air and water.

In air both I_{VM} and I_{hair} make similar contributions to I_{eff} (table 2). In water, however, I_{VM} dominates the contribution to I_{eff}. For the conditions considered in this study, the values for I_{eff} in water are always considerably greater than the corresponding values in air.

The effect of changing hair diameter on I_{eff} in the two media is shown in table 2. By increasing the hair diameter, I_{hair} increases by a larger factor than I_{VM} in both air and water. As I_{eff} in air is more sensitive to changes in I_{hair} than in water, I_{eff} increases proportionately more in air with increasing hair diameter.

The above observations help us interpret hair motion in the two media, as calculated using the theory of damped oscillating systems. It can be shown that the resonance frequency for the hair (the frequency at which the amplitude of the hair is the largest) varies according to $(S/I_{\text{eff}})^{0.5}$. Any change in the value of the resonance frequency changes the hair response to medium oscillations. Therefore, for all conditions

PHILOSOPHICAL TRANSACTIONS OF THE ROYAL SOCIETY B BIOLOGICAL SCIENCES

Table 2. *Values of* I_{VM}, I_{hair} *and* I_{eff} *for two hair diameters and two flow oscillation frequencies for a hair in air and in water*

	d = 7 μm		d = 14 μm	
	f = 10 Hz	f = 500 Hz	f = 10 Hz	f = 500 Hz
in air				
I_{VM} (kg m^2)	4.23×10^{-18}	0.20×10^{-18}	5.55×10^{-18}	0.29×10^{-18}
I_{hair}(kg m^2)	1.76×10^{-18}	1.76×10^{-18}	7.06×10^{-18}	7.06×10^{-18}
$I_{eff} = I_{VM} + I_{hair}$	5.99×10^{-18}	1.96×10^{-18}	12.61×10^{-18}	7.35×10^{-18}
in water				
I_{VM} (kg m^2)	341.22×10^{-18}	21.93×10^{-18}	486.52×10^{-18}	37.48×10^{-18}
I_{hair}(kg m^2)	1.76×10^{-18}	1.76×10^{-18}	7.06×10^{-18}	7.06×10^{-18}
$I_{eff} = I_{VM} + I_{hair}$	342.98×10^{-18}	23.69×10^{-18}	493.58×10^{-18}	44.54×10^{-18}

remaining the same, the resonance frequency for a hair (and therefore its response) in air will differ from that in water according to the value of I_{eff}. Recalling that the values of I_{eff} differ in the two media primarily due to differences in the values for dynamic viscosity, it follows that for the same hair any major differences in hair motion response in air and in water can be attributed to the differences in dynamic viscosities of the two media.

(*iii*) *Hair response*

As $\mu_{water} > \mu_{air}$, I_{eff} in water is larger than in air and the resonance frequency for a hair in water will be lower than in air. This is demonstrated in the calculated results for θ_{max}, the maximum angular displacement, shown in figure 4*a*. The resonance frequency for the hair in air is about 180 Hz, whereas that for the hair in water is 4.1 Hz (not shown in the figure). $\dot{\theta}_{max}$, the maximum angular velocity amplitude, is virtually independent of the oscillation frequency in water. In air, however, the plot shows a peak at about 220 Hz. The maximum angular acceleration amplitude ($\ddot{\theta}_{max}$) depends almost linearly on frequency for the hair in water over the entire frequency range calculated. In air, the angular acceleration of the hair increases up to about 220 Hz and remains nearly constant thereafter.

A comparison of hair displacement and its time derivatives with the corresponding quantities characterizing the flow field oscillations provides information as to which one of the two media allows the hair to more closely follow the movements in the medium. The far field particle displacement amplitude U_0/w, the velocity amplitude U_0, and the acceleration amplitude $U_0 w$ have a striking resemblance to the profiles for hair deflection, velocity and acceleration in water if plotted as functions of frequency. Particle displacement follows a hyperbolic relation, whereas velocity is a constant and acceleration increases linearly with frequency.

To understand the similarity between the shapes of the amplitude plots for the medium and the hair when the flow medium is water, we recall that the boundary layer in water is typically 4.5-fold thinner than in air. This implies that a hair of given length penetrates the boundary layer in water more than the boundary layer in air (for $f = 50$ Hz, $\delta_{water} = 320$ μm, $\delta_{air} = 1432$ μm; for $f = 500$ Hz, $\delta_{water} = 101$ μm, $\delta_{air} = 453$ μm). As a result, the velocity and acceleration profiles contained in the integral terms of equation (3) describing the hair motion can be approximated by constants for the case when the hair ($L = 500$ μm) is in water. With this simplification to equation (3), we can obtain an analytical solution for θ^*_{max}, the maximum dimensionless amplitude of θ^*, in terms of the hair motion parameters G_R, G_S, G_D and G_{VM}. The solution is given by:

$$\theta^*_{max} = \tfrac{1}{2}\sqrt{\{(G_{vm}^2 + G_D^2)/[(G_s - 1)^2 + G_R^2]\}} \qquad (6)$$

For the frequency range shown in figure 4 (50–500 Hz), we can calculate θ^*_{max} as a function of frequency by using the numerical values of the hair motion parameters plotted in figure 3. Owing to space constraints we do not present the plot of θ^*_{max} as a function of frequency but, instead, just mention that in water it is a very slowly decreasing function of frequency (for $f = 50$ Hz, $\theta^*_{max} = 1.53$; and for $f = 500$ Hz, $\theta^*_{max} = 1.46$; a 4.6% change). Therefore, over this frequency range, θ^*_{max} can be assumed to be a constant (C). This implies that, because of the thinner boundary layer in water (effect of kinematic viscosity, ν) *and* due to the observed trends in the values for the hair motion parameters (effect of dynamic viscosity, μ), the functional forms for hair displacement, velocity and acceleration amplitudes are given by CU_0/Lw, CU_0/L, and CU_0w/L, respectively (by using the definitions for the amplitudes given immediately after equation 2). Thus, for a hair in water θ_{max} varies according to a hyperbola, $\dot{\theta}_{max}$ is a constant, and $\ddot{\theta}_{max}$ varies linearly with frequency.

By using the expression $\theta_{max} = CU_0/Lw$ to determine the maximum angular hair displacement, we obtain a value of 2.79° for $f = 50$ Hz (with $C = 1.53$, $L = 500$ μm, and $U_0 = 5$ mm s^{-1}). This is in very good agreement with the value of 2.78° shown in figure 4*a*, which was obtained without making any of the above mentioned simplifications. This agreement provides an additional check for the numerical procedures over and above the checks mentioned in Humphrey *et al.* (1993). Similar agreements are found for the velocity and acceleration amplitudes.

In air, a hair of length $L = 500$ μm remains mostly submerged in the boundary layer for the frequency range $50 \leqslant f \leqslant 500$ Hz. Therefore, simplifications cannot be made to the velocity and acceleration profiles. Even if simplifications were to be made to yield values of θ^*_{max} by using equation (6), these vary from $\theta^*_{max} = 0.25$ at $f = 50$ Hz to $\theta^*_{max} = 0.70$ at $f = 500$ Hz: a

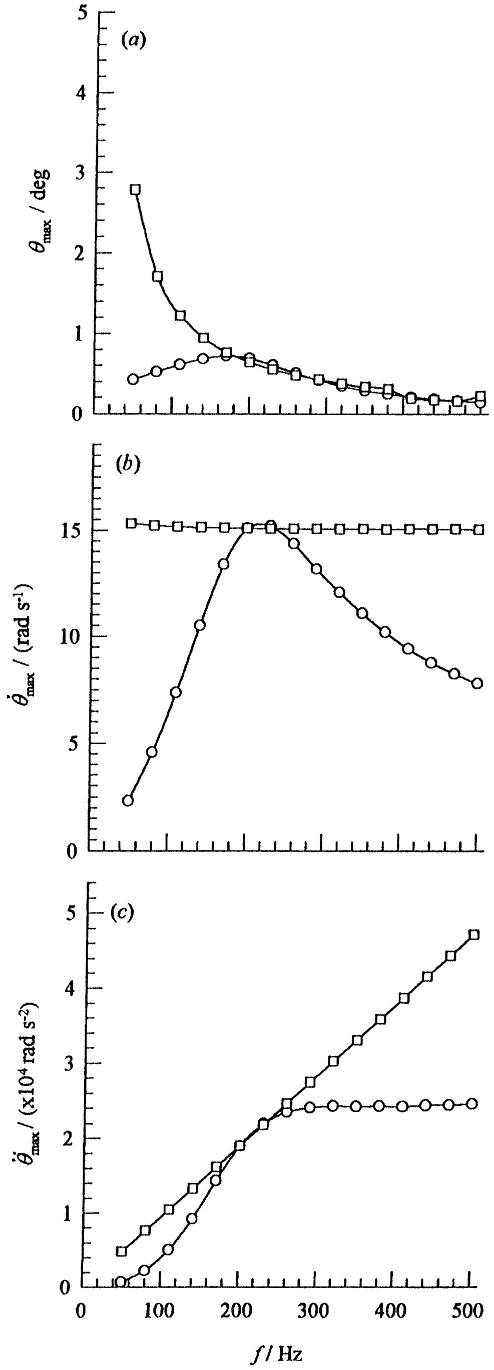

Figure 4. Flow media effects: hair movement response in air (circles) and in water (squares) as a function of flow oscillation frequency. The hair parameters are set to: $L = 500$ µm; $d = 7$ µm; $S = 4 \times 10^{-12}$ N m rad^{-1}; and $R = 0$ N m s rad^{-1}. (*a*) maximum hair angular displacement; (*b*) maximum hair angular velocity; and (*c*) maximum hair angular acceleration.

180% change. Hence, the shape of the plots corresponding to the case of the hair in air cannot be as readily explained through simplified analytical considerations.

In summary, it is clear that the response of a hair to flow field oscillations strongly depends on the fluid medium around it, and that differences in hair response are primarily due to differences in the dynamic viscosity μ for the two media.

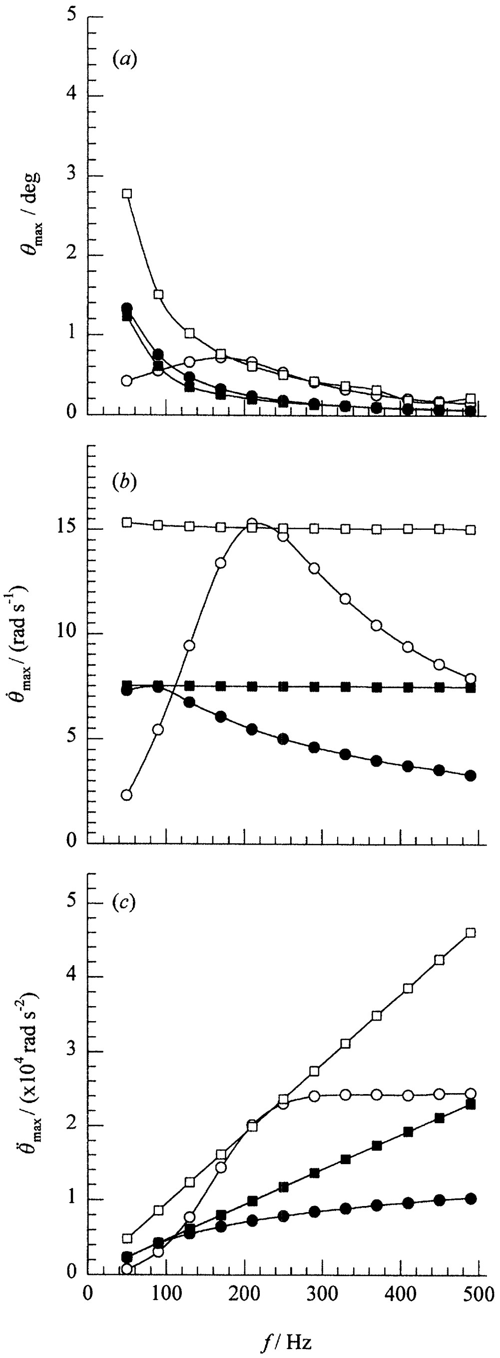

Figure 5. Length effects: hair movement response in air (circles) and in water (squares) as a function of flow oscillation frequency. The hair parameters are set to: $L =$ 500 (open symbols) and 1000 µm, (closed symbols) $d =$ 7 µm, $S = 4 \times 10^{-12}$ N m rad^{-1}, $R = 0$ N m s rad^{-1}. (*a*) maximum hair angular displacement; (*b*) maximum hair angular velocity; and (*c*) maximum hair angular acceleration.

(*b*) *Hair parameter effects*

(*i*) *Length*

Figure 5 shows plots of $\theta^*_{\max}$, $\dot{\theta}_{\max}$ and $\ddot{\theta}_{\max}$ versus frequency for hairs of lengths 500 µm and 1000 µm ($d = 7$ µm, $S = 4 \times 10^{-12}$ N m rad^{-1}, $R = 0$ N m s rad^{-1}) in air and water. Hair responses are different for the two hair lengths in both air and water. As shown by the expressions in Humphrey *et al.* (1993), I_{eff} depends quadratically on hair length L. An increase in

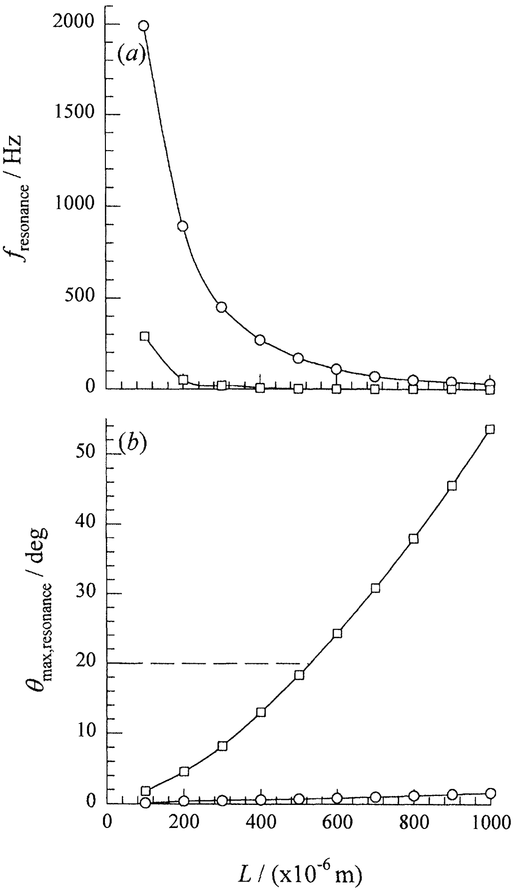

Figure 6. Length effects: plots of (*a*) resonance frequency and (*b*) resonance amplitude as functions of hair length (L) in air (circles) and water (squares). Other hair parameters are set to $d = 7$ μm, $S = 4 \times 10^{-12}$ N m rad^{-1}, $R = 0$ N m s rad^{-1}. Dotted line in (*b*) represents upper theoretical limit for accurate calculations.

hair length will, therefore, significantly increase the moment of inertia, I_{eff}. This, in turn, will shift the resonance frequency to a lower value as shown in figure 5*a* for the two hairs in air.

Although the plots for $\dot{\theta}_{\max}$ and $\ddot{\theta}_{\max}$ also show a dependence of hair response on the length of the hair, the plots in figure 5 do not provide a measure of relative sensitivity to length changes in the two media. To address the sensitivity issue, figure 6 shows plots of resonance frequency and resonance amplitude (representative of the shape of the displacement versus frequency plots) as functions of hair length (obtained for the same values of d, S and R). The resonance frequency is sensitive to changes in hair length for $L <$ 700 μm in air and for $L <$ 200 μm in water (figure 6*a*). Over the range of hair lengths investigated the resonance frequency of hairs in air is more sensitive to changes in hair length. Both in air and water, the resonance frequency decreases and the resonance amplitude (figure 6*b*) increases with increasing hair length. However, the resonance amplitude of hairs in water is more sensitive to increasing hair length than for hairs in air. (It should be noted that the section of the curve representing hair displacements in water with values larger than 20° is only an estimation and not accurate. This is because the mathematical model used for predicting the hair oscillations assumes that the angular displacement of the hair is less than 20°. Notwithstanding, the trend shown in the figure should be qualitatively correct.)

In conclusion, hair response is sensitive to changes in hair length both in air and in water. The resonance frequency of a hair is more sensitive to changes in hair length for hairs in air while the resonance amplitude is more sensitive to changes in hair length for hairs in water.

(*ii*) *Diameter*

To study diameter effects, calculations were performed for two hairs of diameter 7 and 14 μm, respectively, with the remaining parameters unchanged ($L = 500$ μm, $S = 4 \times 10^{-12}$ N m rad^{-1}, $R = 0$ N m s rad^{-1}). Earlier, it was seen that the effect of the medium on hair response is mainly through the term I_{eff} ($= I_{\text{VM}} + I_{\text{hair}}$). Referring to table 2 it can be seen that, by increasing the diameter, I_{hair} increases by a larger factor than I_{VM}. However, if I_{VM} is much larger than I_{hair}, as it is in water, then a change in diameter will not significantly affect I_{eff} and, therefore, the behaviour of the hair.

In air I_{hair} is significant relative to I_{VM} and a change in diameter changes I_{eff} and, therefore, the hair's response (figure 7). In air the maximum displacement resonance frequency of the thicker hair is shifted to a lower frequency, and similar observations can be made for $\dot{\theta}_{\max}$ and $\ddot{\theta}_{\max}$. In contrast, the responses in water are virtually indistinguishable for the two diameters. Thus, the responses of hairs in air are more sensitive to changes in hair diameter than hairs in water, as expected.

(*iii*) *Torsional spring stiffness*

The effect of changing S was investigated by performing calculations for two values of S: 4×10^{-12} and 8×10^{-12} N m rad^{-1}, with the rest of the parameters unchanged ($L = 500$ μm, $d = 7$ μm, $R = 0$ N m s rad^{-1}). Changing S hardly affects the hair response in water but does affect the hair response in air (figure 8). For the air case, the resonance frequencies and, to some extent, the magnitudes of displacement and acceleration depend on S. The calculated dependence of the resonance frequency on S is expected on theoretical grounds, since this is given by $(S/I_{\text{eff}})^{0.5}$. As noted earlier (table 2), I_{eff} is much larger in water than in air and, therefore, in water, unlike in air, changing S by a factor of 2 will not significantly affect the absolute location of the resonance frequency. This is in accordance with the plots in figure 8*a*.

To further investigate the relative sensitivity to changes in S for hairs in air and water, the following question was asked: if a small young hair grows, with molts, into a longer hair, how must S change at the hair base so that resonance is always, say, at 100 Hz? For these calculations, hair length was varied from 100 μm to 1000 μm in steps of 100 μm. Figure 9 shows the change in S required to maintain the resonance frequency at 100 Hz. For the hair in air the rate of change in S with L is of order 10^{-14} N rad^{-1} while for the hair in water it is of order 10^{-12} N rad^{-1}. The

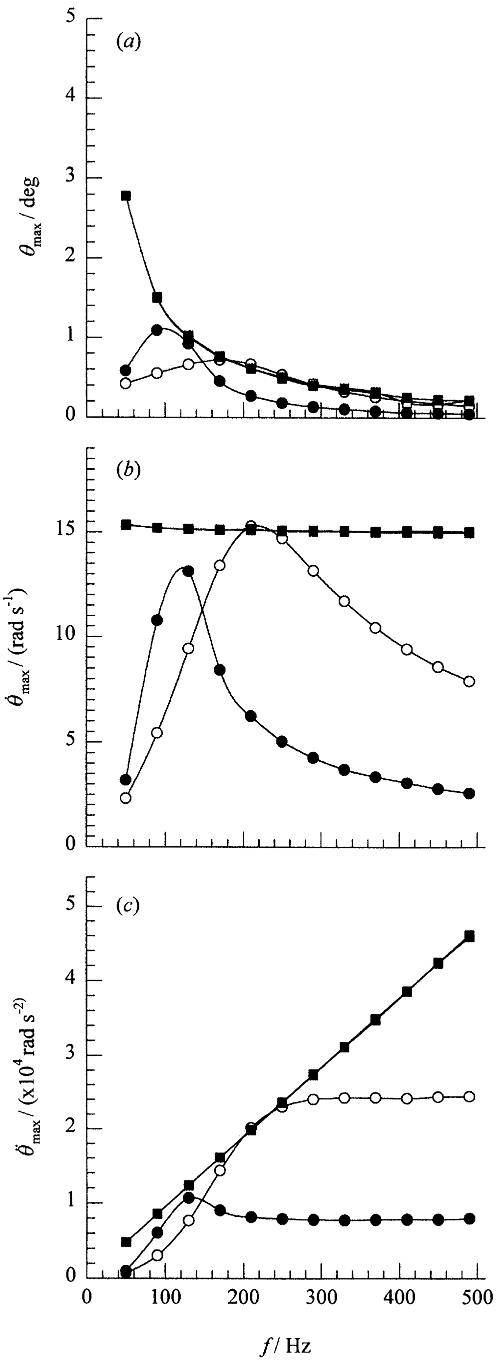

Figure 7. Diameter effects: hair movement response in air (circles) and water (squares) as function of flow oscillation frequency. The hair parameters are set to: $L = 500$ μm, $d = 7$ (open symbols) and 14 μm (filled symbols), $S = 4 \times 10^{-12}$ N m rad^{-1}, $R = 0$ N m s rad^{-1}. (*a*) maximum hair angular displacement, (*b*) maximum hair angular velocity, and (*c*) maximum hair angular acceleration.

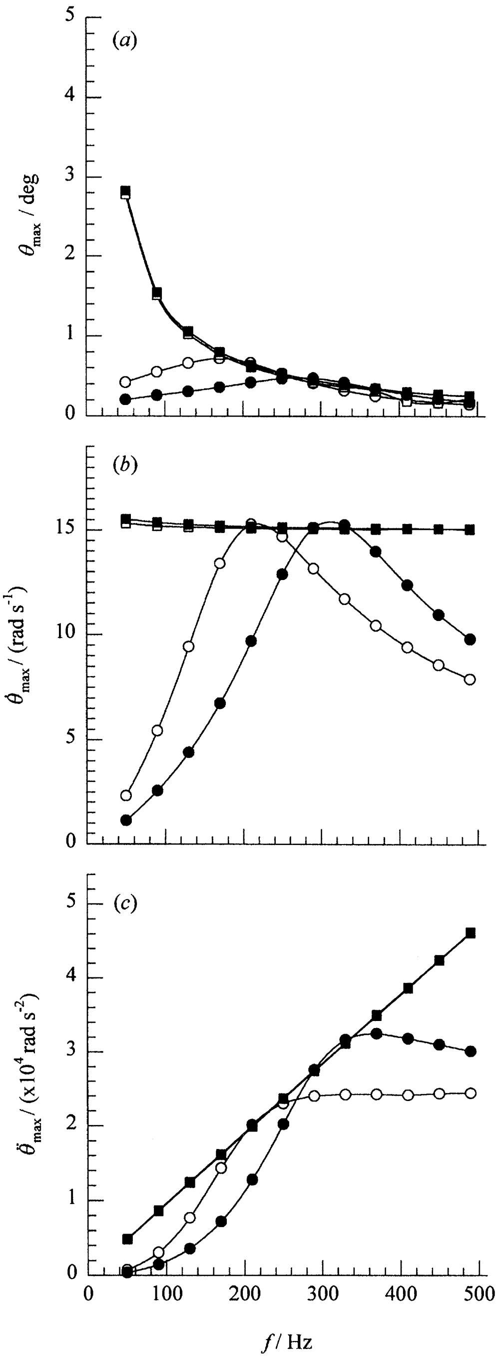

Figure 8. Torsional spring effects: hair movement response in air (circles) and water (squares) as a function of flow oscillation frequency. The hair parameters are set to: $L =$ 500 μm, $d = 7$ μm, $S = 4 \times 10^{-12}$ (open symbols) and 8×10^{-12} N m rad^{-1}, (filled symbols) $R = 0$ N m s rad^{-1}. (*a*) maximum hair angular displacement; (*b*) maximum hair angular velocity; and (*c*) maximum hair angular acceleration.

smaller value for air points to the lower sensitivity in the response of a hair to motion in that medium relative to water.

(*iv*) *Torsional damping*

Four values of R were used to study the effect of changing R on hair response in the two media: 0, 0.01, 0.02 and 0.04 ($\times 10^{-12}$ N m s rad^{-1}) with the rest of the parameters unchanged ($L = 500$ μm, $D = 7$ μm, $S = 4 \times 10^{-12}$ N m rad^{-1}). Both in air and in water the response decreases with increasing R (figure 10). For a change of R from 0.00 to 0.04×10^{-12} N m s rad^{-1}, the response in air is affected to a larger extent than in water for values $f >$ ca. 20 Hz. This shows that the hair motion in air is more sensitive to the value of R than in water. In water, the hair's response is only seen to change at considerably higher values of R and

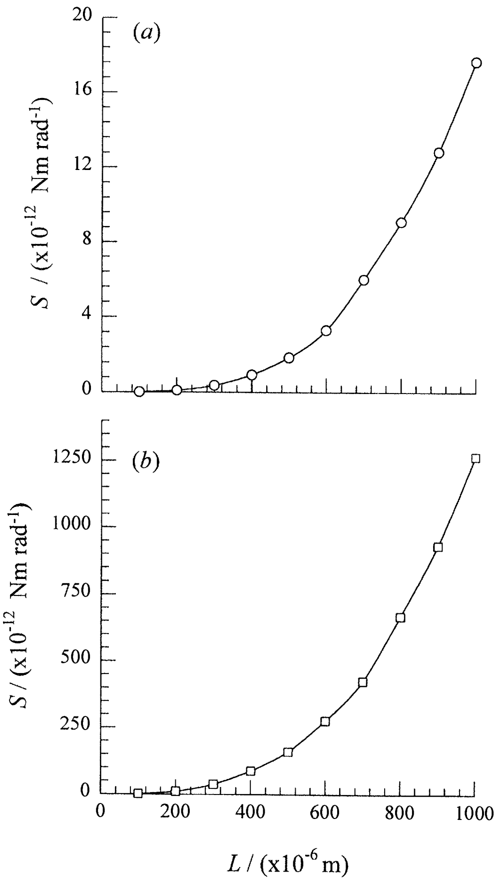

Figure 9. Torsional spring effects: change in the value of torsional spring constant (S) required with change in hair length (L) to maintain the resonance frequency at 100 Hz, in (a) air (circles), and (b) water (squares). Other hair parameters are set to $d = 7$ μm, and $R = 0$ N m s rad^{-1}.

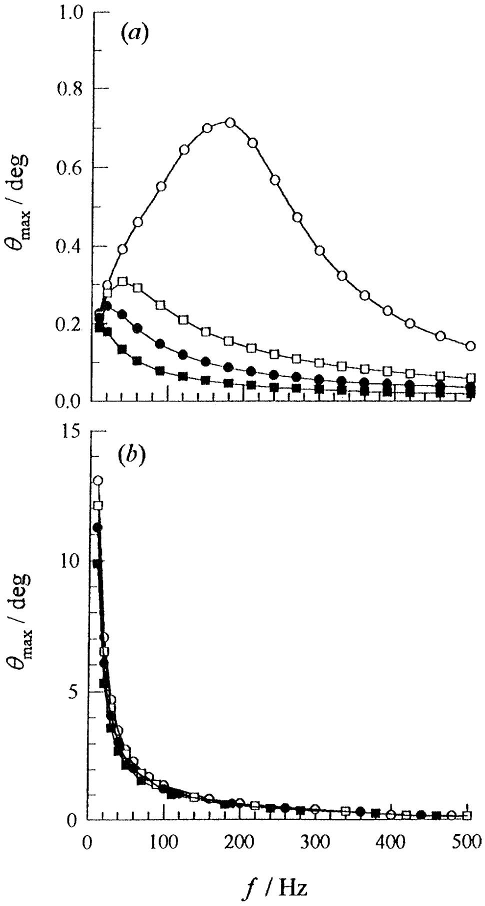

Figure 10. Torsional damping effects: for hair parameters $L = 500$ μm, $d = 7$ μm, $S = 4.0 \times 10^{-12}$ and four values of R. Open circles, air, $R = 0.00 \times 10^{-12}$ N m s rad^{-1}; open squares $R = 0.01 \times 10^{-12}$ N m s rad^{-1}; filled circles $R = 0.02 \times 10^{-12}$ N m s rad^{-1}; filled squares: $R = 0.04 \times 10^{-12}$ N m s rad^{-1}. (a) Maximum hair angular displacement in air, and (b) maximum hair angular displacement in water.

particularly at frequencies below ca. 50 Hz (tested for $R = 0.40 \times 10^{-12}$ N m s rad^{-1}).

(c) *Hair substrate and flow configuration effects*

As we have seen, the hair response depends on the velocity and acceleration profiles established in the boundary layer, and on the hair motion parameters G_R, G_S, G_D and G_{VM}. The latter are independent of substrate-flow configuration characteristics. The differences in hair response to changes in the substrate-flow conditions are, therefore, entirely due to the differences in the velocity and acceleration profiles that are established over the substrate. (These effects are respectively captured by the integral terms in equation 3.)

In addition to the kinematic viscosity (ν) of the fluid medium and the oscillation frequency, the velocity profiles depend on the substrate geometry and its orientation with respect to the plane of fluid oscillations. Humphrey *et al.* (1993) considered three substrate-flow configurations: flat substrate, and cylindrical substrate with axis parallel or perpendicular to the plane of fluid oscillations. In this study only the flat substrate configuration has been extensively investigated. For the case of a cylindrical substrate with its axis parallel to the plane of fluid oscillations, the hair response calculated for a flat substrate is also valid provided the values for substrate diameter D and fluid oscillation frequency f satisfy the condition $fD^2/\nu > 20/\pi$ (see §3*a*i).

For the perpendicular orientation of a cylinder the configuration can never be approximated as a flat plate for any substrate diameter and flow oscillation frequency pair. Humphrey *et al.* (1993) provide the equation describing the velocity profile corresponding to this substrate-flow configuration. Unlike the flat or parallel cases, this case has an asymptotic value for the boundary layer thickness $\delta \gg 4.5D$ for both fluid media. This value of δ is for frequencies greater than 200 Hz. It is larger for lower frequencies. This implies that for a substrate diameter of $D = 1$ mm, a hair of length $L = 500$ μm will be totally submerged in the boundary layer for $f < 500$ Hz. Thus, the substrate geometry and orientation with respect to the plane of fluid oscillations also determine the thickness of the boundary layer and the shapes of the velocity and acceleration profiles contained therein.

As information concerning the shape of the velocity profile in the boundary layer enters the torque balance exclusively via the integral terms in equation (3), the resonance frequency of a hair will not be affected due to changes in the substrate-flow configuration. The amplitudes of hair displacement, velocity and acceleration, however, will be affected as was extensively documented in Humphrey *et al.* (1993).

4. DISCUSSION

Sensitivity to hydrodynamic stimuli is widespread among animals, and is known in most phyla. Accordingly, there are several rather different hydrodynamic receptor systems. These include the lateral line and free neuromast systems of fish and amphibians, the epidermal lines of cephalopods, and all kinds of hair-like structures found on the body surface of animals of such different taxonomic affiliation as arthropods, molluscs and chaetognaths (Budelmann 1989; Bleckmann 1994).

Among the aquatic arthropods cuticular sensory hairs have received most attention in decapod crustaceans. Their body surface may be covered by thousands of cuticular hairs. Many of these hairs are likely to be tactile and/or both mechano- and chemosensitive. The most typical hydromechanic receptors among the decapod crustacean hairs are the pit hairs and the peg sensilla (Laverack 1962*a*, *b*; Tautz & Sandeman 1980; Derby 1982). However, morphologically less specialized hairs were found to be sensitive to water movement as well (Wiese 1976; Breithaupt & Tautz 1990). Considering the difference between the physical properties of air and water and the results of this paper we may now ask whether there are any distinct differences in morphology and mechanics to be expected for hairs sensitive to air and water movement, respectively.

(*a*) *Boundary layer thickness*

In water, boundary layer thickness (δ) is smaller than in air, due to the smaller value for its kinematic viscosity. A straightforward conclusion from this seems to be that hairs sensitive to hydrodynamic stimuli may be shorter than hairs sensitive to air movement and still pick up a signal or even protrude into the region of free flow velocity. When comparing actual hairs one has to be more specific and consider several parameters, however.

Whereas the dynamic viscosity of water at 27 °C is about 43-fold larger than that of air (because of the much smaller density of air), the kinematic viscosity (dynamic viscosity over density) of air is about 20-fold larger than that of water. Boundary layer thickness δ is given by $\delta_{\text{air}} = 2.54\ (\nu_{\text{air}}/f)^{0.5}$ for air and by $\delta_{\text{water}} = 2.54\ (\nu_{\text{water}}/f)^{0.5}$ for water. It follows that $\delta_{\text{air}} = \delta_{\text{water}}\ (\nu_{\text{air}}/\nu_{\text{water}})^{0.5}$ or, using the data, that $\delta_{\text{air}} = 4.46\delta_{\text{water}}$. For a medium oscillating at 150 Hz, δ_{air} is calculated to be 827 μm, whereas δ_{water} is 186 μm. According to an older statement in the literature related to crustacean hairs, boundary layer thickness in water is quoted as being 1000-fold smaller than in air (Tautz & Sandeman 1980). This statement has to be revised.

It can be shown that the absolute difference between the boundary layer thickness in air and in water for a flow oscillating perpendicular to a cylinder (such as a body appendage) is larger than it is for a flat substrate or a cylinder in parallel orientation to the flow. This effect increases with increasing flow oscillation frequency.

(*b*) *Reynolds and Strouhal numbers*

The expression $\delta = 2.54\ (\nu/f)^{0.5}$ can be manipulated to yield $\delta/l = 2.54\ St^{-0.5}Re^{-0.5}$ where $St = fl/u$ and $Re = u\ l/\nu$, u and l being the characteristic velocity and length scales in the flow. Thus, we see that boundary layer thickness typically decreases with increasing Reynolds number (*Re*) or Strouhal number (*St*). Because for equal l and u *Re* is larger in water than in air (for fixed *St* number), the boundary layer thickness should be smaller in water.

Because kinematic viscosity is smaller by a factor of about 20 in water relative to air, for geometrically similar hairs the same *Re* is found at movement velocities 20-fold smaller in water compared to air. According to Vogel (1989), movement velocities in water are indeed smaller than in air by roughly this amount and the result would be that hairs operate at roughly the same *Re* in both media. At the same *Re* a given hair in water will still experience a larger drag force compared to air because drag force is a function of dynamic viscosity μ ($\mu_{\text{water}} = 8 \times 10^{-4}$ kg m^{-1} s^{-1}, $\mu_{\text{air}} = 1.85 \times 10^{-5}$ kg m^{-1} s^{-1}).

(*c*) *Hair length*

There is a good reason then why a hair sensitive to hydrodynamic stimuli may indeed be shorter than a hair in air and still have the same mechanical sensitivity: namely, the larger drag force per unit length, and the smaller boundary layer thickness which, for the same value of velocity amplitude, also implies a higher shear rate (steeper velocity gradient).

The crustacean cuticular hairs considered to be the most typical hydrodynamic receptors are the so called peg sensilla (Laverack 1962*a*, *b*; Bush & Laverack 1982; Derby 1982). They are indeed the stumpy, very short hair sensilla one would predict considering the above argument. In the lobster, *Homarus vulgaris*, peg sensilla on the pereiopods are composed of a solid central rod from which branches extend. The rod is only about 30 μm long (70 μm in a second type of peg sensillum) (Derby 1982). Peg sensilla lying in a shallow depression of the cuticular surface are known in many species of crustaceans. A particularly high density of about 75 cm^{-2} was noted for the lobster chelae (Laverack 1962*a*, *b*). The German term 'Büschelorgan' coined by Luther (1930) as well as the term 'hair fans' (Laverack 1962*a*, *b*) and 'pinnate hairs' (Tazaki & Ohnishi 1974) for hair sensilla identical or similar to peg sensilla describe the prominent featheriness. Most likely there are also mechanoreceptors among the shortest crustacean cuticular hairs which are only 20 μm long (Tautz & Sandeman 1980; Derby 1982).

Despite this agreement between the shape of hydrodynamic receptors with our expectations derived from theory, it has to be emphasized that hydrodynamic sensitivity in crustaceans is not restricted to hairs of such tiny length. In crayfish, responses to hydrodynamic stimuli are described by various authors for hairs ranging in length from 300 μm to 1000 μm (Wiese 1976), up to 300 μm (Breithaupt & Tautz 1990), and from 75–500 μm (Tautz & Sandeman 1980). Vedel & Clarac (1976) attribute hydrodynamic sensitivity to sensilla similar to peg sensilla and from 150–300 μm long. The longest hairs to be quoted in this context are feathered hairs on the edge of the lobster swimmeret ramus. They are from 2–4000 μm long and suggested to be sensitive to large amplitude water displacements produced by the motion of the rami themselves (Killian & Page 1992).

The conclusion from all this is that we do find the very short hairs expected in aquatic arthropods. Their length does indeed remind us of the cilia taking up water movement stimuli in many aquatic animals (e.g. primary sensory cells of the cephalopod epidermal lines: Bleckmann *et al.* 1991*b*; ciliated cells on the leech body surface: McVean *et al.* 1991; lateral line hair cells of anamniotic vertebrates including those of free-standing neuromasts: review Bleckmann 1994). Equally important, the most typical hydrodynamic receptors seem to be shorter than the most typical aerodynamic receptors i.e. insect thread hairs and arachnid trichobothria, which are between about 100–3000 μm long (cricket cercal thread hairs up to 3000 μm: Gnatzy & Schmidt 1971; scorpion trichobothria up to 1800 μm: Meßlinger 1987; bird spider trichobothria up to 2500 μm: Den Otter 1974; wandering spider trichobothria up to 1400 μm: Barth *et al.* 1993). The existence of rather long hydrodynamic receptor hairs should not surprise us since hair length is only one among several parameters determining a hair's mechanical sensitivity (Humphrey *et al.* 1993). Also, different hairs are exposed to different medium movements and, therefore, are likely to serve different ranges of sensitivity.

(*d*) *Hair diameter*

Whereas the length of a hair considerably influences its mechanical sensitivity in both air and water, our results predict only a minor influence of hair diameter on this quantity in water compared to air. The main reason for this is the much larger moment of inertia due to virtual mass in water compared to that of the hair proper. As a consequence we may speculate that the evolutionary selective pressure on hair diameter may have been smaller in aquatic than in terrestrial arthropods. Filiform hairs serving as aerodynamic receptors share very similar morphologies and are characterized by their small diameter of only a few μm (Tautz 1979; Reißland & Görner 1985; Barth *et al.* 1993), the variation of which significantly affects absolute mechanical sensitivity and resonance frequency (figure 6). By comparison, the morphologies of crustacean hydrodynamic hairs appear to vary to a considerably larger extent (see above) and thus may indeed support the prediction of the relative unimportance of hair diameter.

(*e*) *Frequency*

Hydrodynamic receptors are generally considered to be low frequency sensors, that is low-pass filters with a working range between less than 1 Hz and about 150 Hz. This property seems well matched to the frequencies predominating in natural stimuli such as the water movements generated by aquatic animals (Bleckmann 1994). In these signals higher frequency components (up to about 150 Hz) are often superimposed on very low frequencies or even flows of constant velocity.

Whereas in some receptors physiological threshold values follow water flow velocity, they follow acceleration in others (Bleckmann 1994). This difference is thought to go along with the selective preference for different types or components of stimuli: velocity detectors are more adequate for sensing low frequency or even constant-velocity flows, whereas acceleration detectors are more appropriate for the high frequencies which often go along with high acceleration values. The same argument applies for air movement detectors as well which are known to be mechanically more sensitive to velocity or to acceleration, depending on their length (long versus short hairs) (Shimozawa & Kanou 1984*a*, *b*; Barth *et al.* 1993).

(*i*) *The medium*

Our present results, however, point to several significant differences regarding the tuning of filiform hairs in water and in air, respectively. The main reason for these differences is the overriding contribution of I_{VM} to I_{eff} in water as opposed to air.

1. One of the consequences of this is the considerably lower mechanical resonance frequencies for displacement in water than in air (figure 3). Depending on their length, spider trichobothria were found to be mechanically tuned to frequencies between 40 and 600 Hz (Barth *et al.* 1993), and a filiform hair of a caterpillar had its resonance at around 150 Hz (Tautz 1977, 1979). Unfortunately, equivalent measurements are still not available for hairs of aquatic arthropods.

2. Another consequence of the high values for the inertia due to virtual mass in water is the striking constancy of maximum velocity within the frequency range tested (less than 1 Hz to 500 Hz) which is in obvious contrast to the hair in air. Maximum acceleration also does not reveal a resonance in water within the same frequency range which covers all frequencies of biological significance. Instead it rises linearly with stimulus frequency.

It was argued earlier (see §3*a*iii) that a hair ($d = 7$ μm, $L = 500$ μm, $S = 4.0 \times 10^{-12}$ N m rad^{-1}, $R = 0$ N m s rad^{-1}) on a flat substrate follows water movements more closely than air movements. Even though we focussed on a sinusoidal variation in time for the fluid velocity, the importance of I_{VM} in determining the hair response in water is a very general finding. The resonance frequencies for hairs in water can be expected to have lower values than those for hairs in air. Therefore, the hairs in water amplify low frequency movements, and the hairs in air amplify high frequency movements.

In addition to the substrate and hair characteristics, hair motion amplitudes also depend on the frequency spectrum of the stimulus. Usually, both airborne and waterborne disturbances caused by prey or predator and reaching the hairs have much of their energies concentrated in the lower frequencies ($f \approx 10$ Hz) of the spectrum (Bleckmann *et al.* 1991; Barth *et al.* 1995). This characteristic of the stimuli spectra together with the motion characteristics of a hair in air enable large hair deflections over a wide range of frequencies. Because of the large values of moment of inertia in water, the same hair will function better as a displacement detector at low frequencies and as an acceleration detector at higher frequencies. In air, this frequency differentiation is achieved by different length hairs functioning as displacement, velocity and acceleration detectors over different frequency ranges (Shimozawa & Kanou 1984; Kämper & Kleindienst 1990; Barth *et al.* 1993; Humphrey *et al.* 1993).

In concluding this section we note that the power required to drive a hair in water differs from that necessary to drive the same hair in air. This can be shown (using order of magnitude estimates) by recognizing that power is equal to torque times angular velocity. The total torque acting on a hair is $T = T_D + T_{VM}$ and the hair angular velocity is $\dot{\theta}$ (equation 1). Thus, the power required to drive the hair is $P = T \times \dot{\theta}$. Expressions for T_D and T_{VM} are given in Humphrey *et al.* (1993). An inspection of these shows that the dominant contribution to $T_D + T_{VM}$ has the form $C\,\mu$ where μ is the dynamic viscosity of the fluid medium and the value of C can be taken as essentially constant (but different for each fluid medium) for the purpose of the argument presented here. It follows that the power ratio for a hair in water versus the same hair in air is $P_{WAT}/P_{AIR} = (C_{WAT}\ \mu_{WAT}\ \dot{\theta}_{WAT})/(C_{AIR}\ \mu_{AIR}\ \dot{\theta}_{AIR})$. However, if it is required that the frequency, relative velocity and relative acceleration of the hair be the same in both media, then $C_{WAT} = C_{AIR}$. If it is further required that the hairs possess the same absolute angular velocity in both media, then $\dot{\theta}_{WAT} = \dot{\theta}_{AIR}$. Under these restrictive conditions the expression for the power ratio simplifies to $P_{WAT}/P_{AIR} = \mu_{WAT}/\mu_{AIR}(= 43 \text{ at } 27\ °\text{C})$. In practice, hairs in water may be much shorter than hairs in air, as we have seen. This significantly reduces the power requirements to drive them.

(ii) *Hair geometry*

Apart from the medium itself, the geometry of the hair affects its mechanical operation differently in air and in water. Thus the movement of hairs in air is more sensitive to changes in hair length and hair diameter than that of hairs in water. In water, however, amplitude at resonance is much more influenced by hair length than in air, contrasting the effect on resonance frequency.

In agreement with the general tendency stated above S (spring stiffness) and R (torsional damping) are much more influential on a hair's resonance frequency in air than they are in water.

We are thus again left with the idea that the evolutionary pressure on both the morphological parameters and S and R must have been bigger in air than in water, allowing for more diversity in water with much less dramatic effects on mechanical properties. It may be then, that the hairs operating in water are associated with narrower physiological filters. This, however, is speculation and underlines the need for both broad and detailed, and comparative analyses of individual cases of arthropod hydrodynamic hair receptors, considering hair mechanics, physical properties of the relevant stimuli, as well as the physiological responses of the sensory cells. For filiform hairs operating in air it seems well documented that the response properties of the sensillum are largely under the influence of the hair and air mechanics (Tautz 1977, 1979; Shimozawa & Kanou 1984; Kämper & Kleindienst 1990; Barth *et al.* 1993; Humphrey *et al.* 1993).

Generously supported by the Austrian Science Foundation FWF through a Lise-Meitner postdoctoral fellowship to R.D. and grant P 9336-BIO to F.G.B. J.A.C.H. gratefully acknowledges support received from the office of the Vice President for Research at the University of Arizona through the Small Grants Program. Thanks are also due to R. Sudarsan for some of the calculations leading to figure 10, and to M. Wieser for perfect secretarial assistance.

REFERENCES

Barth, F. G. 1986 Zur Organisation sensorischer Systeme: die cuticularen Mechanoreceptoren der Arthropoden. *Verh. Dtsch Zool. Ges.* **79**, 69–90.

Barth, F. G., Wastl, U., Humphrey, J. A. C. & Devarakonda, R. 1993 Dynamics of arthropod filiform hairs. II. Mechanical properties of spider trichobothria (*Cupiennius salei* Keys.). *Phil. Trans. R. Soc. Lond.* B **340**, 445–461.

Barth, F. G., Humphrey, J. A. C., Wastl, U., Halbritter, J. & Brittinger, W. 1995 Dynamics of arthropod filiform hairs. III. Flow patterns related to air movement detection in a spider (*Cupiennius salei* Keys.). *Phil. Trans. R. Soc. Lond.* B **347**, 397–412.

Bleckmann, H., Breithaupt, T., Blickhan, R. & Tautz, J. 1991 The time course and frequency content of hydrodynamic events caused by moving fish, frogs, and crustaceans. *J. comp. Physiol.* A **168**, 749–757.

Bleckmann, H. 1994 *Reception of hydrodynamic stimuli in aquatic and semiaquatic animals.* Stuttgart, Jena, New York: G. Fischer.

Breithaupt, T. & Tautz, J. 1990 The sensitivity of crayfish mechanoreceptors to hydrodynamic and acoustic stimuli. In *Frontiers in crustacean neurobiology* (ed. K. Wiese, W.-D. Krenz, J. Tautz, H. Reichert & B. Mulloney), pp. 114–120. Basel: Birkhäuser.

Budelmann, B. U. 1989 Hydrodynamic receptor systems in invertebrates. In *The mechanosensory lateral line. Neurobiology and evolution* (ed. S. Coombs, P. Görner & H. Münz), pp. 607–632. New York: Springer.

Bush, B. M. H. & Laverack, M. S. 1982 Mechanoreception. In *The biology of Crustacea*, vol. III (ed. H. L. Atwood & D.C. Sandeman), pp. 399–468. New York: Academic Press.

Den Otter, C. J. 1974 Setiform sensilla and prey detection in the bird-spider *Sericopelma rubronitens* Ausserer (Araneae, Theraphosidae). *Neth. J. Zool.* **24**, 219–235.

Derby, I. 1982 Structure and function of cuticular sensilla of the lobster *Homarus americanus*. *J. Crust. Biol.* **2**, 1–21.

Fletcher, N. H. 1978 Acoustical response of hair receptors in insects. *J. comp. Physiol.* **127**, 185–189.

Gnatzy, W. & Schmidt, K. 1971 Die Feinstruktur der Sinneshaare auf den Cerci von *Gryllus bimaculatus* Deg. (Saltatoria, Gryllidae) *Z. Zellforsch.* **122**, 190–209.

Humphrey, J. A. C., Devarakonda, R., Iglesias, I. & Barth, F. G. 1993 Dynamics of arthropod filiform hairs. I. Mathematical modelling of the hair and air motions. *Phil. Trans. R. Soc. Lond.* B **340**, 423–444.

Kämper, G. & Kleindienst, H.-U. 1990 Oscillation of cricket sensory hairs in a low frequency sound field. *J. comp. Physiol.* A **167**, 193–200.

Killian, K. A. & Page, C. H. 1992 Mechanosensory afferents innervating the swimmerets of the lobster. II. Afferents activated by hair deflection. *J. comp. Physiol.* A **170**, 501–508.

Laverack, M. S. 1962*a* Responses of cuticular sense organs of the lobster, *Homarus vulgaris*. I. Hair–peg organs as water current receptors. *Comp. Biochem. Physiol.* **5**, 319–325.

Laverack, M. S. 1962*b* Responses of cuticular sense organs of the lobster, *Homarus vulgaris*. II. Hair–fan organs as pressure receptors. *Comp. Biochem. Physiol.* **6**, 137–145.

Luther, W. 1930 Versuche über die Chemorezeption der Brachyuren. *Z. vergl. Physiol.* **12**, 177–205.

Meßlinger, K. 1987 Fine structure of scorpion trichobothria (Arachnida, Scorpiones). *Zoomorphology* **107**, 49–57.

Reißland, A. & Görner, P. 1985 Trichobothria. In *Neurobiology of arachnids* (ed. F. G. Barth), pp. 138–161. Berlin: Springer.

Shimozawa, T. & Kanou, M. 1984*a* Varieties of filiform hairs: range fractionation by sensory afferents and cercal interneurons of a cricket. *J. comp. Physiol.* A **155**, 485–493.

Shimozawa, T. & Kanou, M. 1984*b* The aerodynamics and sensory physiology of range fractionation in the filiform sensilla of the cricket *Gryllus bimaculatus*. *J. comp. Physiol.* A **155**, 495–505.

Stokes, G. G. 1851 On the effect of the internal friction of fluids on the motion of pendulums. *Trans. Camb. Phil. Soc.* **9**, 8ff. (Reprinted in *Mathematical and physical papers*, vol. III, pp. 1–141, Cambridge University Press, 1901.)

Tautz, J. 1977 Reception of medium vibration by thoracal hairs of caterpillars of *Barathra brassicae* L. (Lepidoptera, Noctuidae). I. Mechanical properties of the receptor hairs. *J. comp. Physiol.* **118**, 13–31.

Tautz, J. 1979 Reception of particle oscillation in a medium. An unorthodox sensory capacity. *Naturwissenschaften* **66**, 452–461.

Tautz, J. & Sandeman D. C. 1980 The detection of waterborne vibration by sensory hairs on the chelae of the crayfish. *J. exp. Biol.* **88**, 351–356.

Tazaki, K. & Ohnishi, M. 1974 Responses from tactile receptors in the antenna of the spiny lobster *Panulirus japonicus*. *Comp. Biochem. Physiol.* A **47**, 195–199.

Vedel, J. P. & Clarac, F. 1976 Hydrodynamic sensitivity by cuticular organs in the rock lobster *Panulirus vulgaris*. Morphological and physiological aspects. *Mar. Behav. Physiol.* **3**, 235–251.

Vogel, S. 1989 *Life in moving fluids. The physical biology of flow.* Princeton University Press.

Wiese, K. 1976 Mechanoreceptors for nearfield water vibrations in crayfish. *J. Neurophysiol.* **39**, 816–833. Princeton University Press.

Received 8 December 1995; accepted 5 February 1996